Applied Surface Science 478 (2019) 737–743

Contents lists available at ScienceDirect

Applied Surface Science

journal homepage: www.elsevier.com/locate/apsusc

Full length article

Hierarchical micro/nanostructured TiO_2/Ag substrates based on femtosecond laser structuring: A facile route for enhanced SERS performance and location predictability

Jinlong Lu[a], Jianjun Yang[a], Subhash C. Singh[a,b], Zhibing Zhan[b], Zhi Yu[a], Wei Xin[a], Ting Huang[c,*], Chunlei Guo[a,b,**]

[a] The Guo China-U.S. Photonics Lab, Changchun Institute of Optics, Fine Mechanics, and Physics, Changchun 130033, China
[b] The Institute of Optics, University of Rochester, Rochester, NY 14627, USA
[c] High-power and Ultrafast Laser Manufacturing Lab, Institute of Laser Engineering, Beijing University of Technology, Beijing 100124, China

ARTICLE INFO

Keywords:
Femtosecondlaser
Chemical treatment
Hierarchical micro/nanostructured TiO2/Ag
SERS

ABSTRACT

Hierarchical micro/nanostructured TiO_2/Ag substrates for surface-enhanced Raman scattering (SERS) application are fabricated by depositing Ag nanoparticles on the surface of TiO_2 hierarchical micro/nanostructures, which are formed by combining femtosecond laser structuring with scalable hydrothermal treatment. Our results show that the morphology of hierarchical micro/nano TiO_2/Ag architectures can significantly influence SERS performance. Compare with one-dimensional TiO_2/Ag nanostructures hydrothermally fabricated on laser untreated Ti surface, a four-fold enhancement is shown in the SERS signal with excellent reproducibility. Most importantly, enhancement is significantly stronger in the valleys of our microstructures than on the hills due to geometrical orientation of nanostructures on the surface of the microstructure. The site predictability for SERS enhancement is one of the major roadblock for SERS applications. Present study provides an effective way to enhance the site predictability for optimal SERS in addition to a significant enhancement in signal strength.

1. Introduction

Due to its supersensitivity, selectivity, and rapid response, surface enhanced Raman scattering (SERS) spectroscopy is recognized as one of the most promising analytical tools for applications in various fields, such as analytical chemistry, life science, medical science, and the identification of trace chemical species with limit-of-detection up to single molecular level [1–5]. It has generally been accepted that SERS is mainly attributed to the electric field enhancement of incident light at the surface of metallic nanostructures with strong surface plasmon resonance (SPR) absorption, and noble metal nanostructures are renowned and widely used due to their better performance [6–8]. But considering the high cost of the noble metals, metal oxide (especially TiO_2) nanostructures coated by a thin layer or functionalized with nanoparticles (NPs) of noble metal are widely used in recent years due to the possibility of fabricate reusable SERS substrates with comparable sensitivity [9–13].

On the other hand, a large number of SERS substrates with various structures and morphologies have been designed and fabricated [8–14]. Among these structures, three-dimensional hierarchical micro/nanostructures with special morphologies and unique properties have attracted considerable attention [14–18]. These structures have larger surface area to adsorb more probe molecules and possess potential to further expand the arrangement of hotspots along the three-dimensional structures, which are both beneficial for the improvement of SERS sensitivity [14–17]. Currently, fabrication of SERS substrates with hierarchical micro/nanostructures typically based on either top-down or bottom-up method [17–20]. Although the former, such as electron-beam lithography (EBL), focused-ion-beam (FIB), or plasma based etching etc. can provide precise control over the design and fabrication of micro-sized structures. These are multi-step, slower, costly and complex procedures [17,20]. Otherwise, bottom-up approaches including self-assembly or aggregation of NPs as building blocks are preferable, but it is difficult to achieve large scale SERS substrate with high uniformity [16,20].

Furthermore, past studies of SERS have focused on their signal enhancement, substrate uniformity, and signal reproducibility. However, little was done on studying the site reproducibility in optimal SERS

* Corresponding author.
** Correspondence to: C. Guo, The Guo China-U.S. Photonics Lab, Changchun Institute of Optics, Fine Mechanics, and Physics, Changchun 130033, China.
E-mail addresses: huangting@bjut.edu.cn (T. Huang), guo@optics.rochester.edu (C. Guo).

https://doi.org/10.1016/j.apsusc.2019.01.257
Received 11 October 2018; Received in revised form 15 December 2018; Accepted 28 January 2019
Available online 29 January 2019
0169-4332/

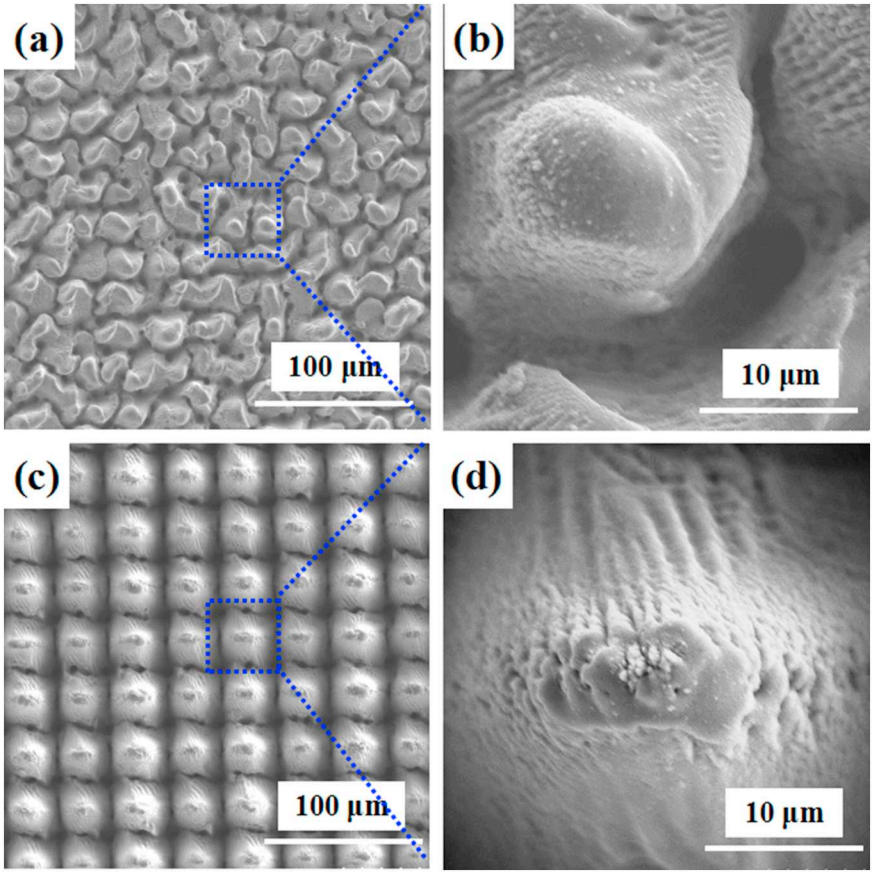

Fig. 1. SEM images of Ti surface after femtosecond laser structuring and fabricate nanostructure TiO_2. (a, b) random structure, (c, d) uniform structure.

enhancement. Therefore, the maximum SERS signal is often found after extensive searching and the optimal site predictability is lacking. In fact, it is extremely important to have this location predictability for the maximum enhancement, especially when the substrate is unknown [22].

Recently, femtosecond laser structuring attracts a great amount of interest for the fabrication of SERS-active substrate by utilizing its unique advantages of flexibility, precise structuring, and controllability to obtain a large variety of micro-structured surfaces [23–30]. It is a much faster and cheaper way than other top-down approaches in the fabrication of microstructured patterns. However, it's nearly impossible to use this method to fabricate three-dimensional hierarchical micro/nanostructures or specific functional materials. Based on the advantages of femtosecond laser structuring, we report on the fabrication of hierarchical micro/nanostructured TiO_2/Ag substrates using a hybrid physicochemical approach by combinating femtosecond laser structuring of Ti substrate with scalable hydrothermal treatment. This hybrid method enables us to synthesize hierarchical micro/nanostructures with good uniformity, reproducibility, and most importantly an excellent site predictability to obtain the optimal SERS signal in an unknown substrate.

2. Experimental section

2.1. Fabrication of TiO_2/Ag substrates

For the fabrication of hierarchical TiO_2 nanostructures using hybrid physico-chemical approach combining femtosecond laser structuring and hydrothermal treatments, we followed our previously work [28]. Namely, Ti sheets (99.99 wt% in purity) were structured by a femtosecond laser system (TRUMPF TRUMICRO 5000), which generates laser pulses with a central wavelength of 1030 nm, 800 fs pulse width, and 400 kHz repetition rate. A scanning galvanometer suitable for the laser system was used to control the scanning motion of the laser beam with high speed and create many kinds of large scale microstructures on Ti surface. Scanning rate of 500 mm/s was chosen for both kinds of structures (scanning interval of 20 and 30 µm for random and uniform structure respectively). The Gaussian beam output from the laser system after focusing at the *1/e*-level has a spot size of ~40 µm. After that, the laser treated Ti sheets with microstructures were ultrasonic cleaned and hydrothermally treated at 220 °C reaction temperature in a Teflon lined stainless steel autoclave containing molar solution of NaOH. After reaction for 4 h, the Ti sheets were immersed in 1 mol/L HCl solution for 10 min. Finally, the specimens were rinsed with distilled water and annealed at 600 °C for 3 h in air using a muffle furnace, which has been proved to be a better condition for SERS application [9]. Ag NPs film with a thickness of 20 nm was deposited on the top of the as-received TiO_2 nano-microstructures through a high vacuum resistance evaporation coating machine (BEIJING TECHNOL CO., LTD. ZHD400).

2.2. Material characterizations

Scanning electron microscope (SEM, PHENOM-WORLD, PHENOM PRO) was used to examine the morphology of the Ti sample at different steps. X-ray diffraction (XRD, BRUKER D8 ADVANCE) measurement was done in the range of 20–80° using Cu-Kα line of λ = 1.5406 A°. XPS data were collected using an X-ray photoelectron spectrometer (XPS, PHI 5300) at a pass energy of 30 eV using the step size of 0.05 eV.

2.3. SERS measurements and recycling SERS performance

For SERS spectral examination, the Ag/TiO_2 substrates were separately soaked in Rhodamine 6G (R6G) ethanol solution with different concentration for 1 h, and dried in the air followed by measurements of SERS spectra using a Raman spectrometer (HORIBA SCIENTIFIC, LABRAM HR EVOLUTION). The incident laser with a wavelength of 532 nm was chosen in our experiment, where total accumulation time for Raman spectra measurements was 20 s under laser power of 2 mW.

For recyclable SERS performance, after each test, the sample was immersed in deionized water and irradiated with a 500 W Xe lamp for 90 min. Then the substrate was washed with deionized water for several times to remove residual ions and molecules during degradation and dried in the air for next time reusing. During the self-cleaning process, the SERS spectra were also recorded after irradiated every 30 min.

3. Result and discussion

Femtosecond laser structuring as one of the most actively studied approaches for surface micro-/nanostructuring receives much attention in recent years due to its high-precision, limitation of heat effect, and flexibility. A large variety of structures can be easily fabricated just through adjusting femtosecond laser parameters (laser power, laser pulse number, and scanning method). Based on this strategy, random (10 μm scanning interval) and uniform (30 μm scanning interval) structures produced by femtosecond laser (Fig. 1) were used in our study, and the name remained unchanged in the whole experiments at different steps. These structures are mainly consisting of femtosecond laser ablated microstructures, laser-induced periodic subwavelength structures and NPs.

Accordingly, as shown in Fig. S1, two types of TiO_2 with different microstructures but similar nanostructures are obtained here due to the same chemical treatment condition. One-dimensional nanostructures are hydrothermally grown and form “flower-like” structures at the surface of microstructures fabricated by femtosecond laser. For their formation, a dissolution-recrystallization process is dominated during this entire hydrothermal process, where Ti on the outside surface is acted as Ti source for the growth of TiO_2 as well as a substrate. During this process, Ti atoms on the outside surface react with NaOH to form a layer of $Na_2Ti_2O_5{\cdot}H_2O$ nanocrystallines on the substrate. At the same time, Ti atoms in the volume could diffuse to the surface to supply source material, which causes the oriented growth of nanorod to form “flower-like” architectures on a curved surface [28–30]. XRD results in Fig. S2 also confirm the formation of intermediate compounds during the fabrication of nanostructure TiO_2 through the hydrothermal process. It is notably that hydrothermal reaction in NaOH solution does not dramatically change the microstructure fabricated by femtosecond laser structuring, and the morphology of nanostructures on the surface of microstructures remained unchanged in the following ion-exchange and annealing process, which ensure the preparation of hierarchal micro-/nanostructures in varied forms just through laser parameter adjustment (results comparison between Figs. S1 and 1).

Silver NPs were deposited on the surface of hierarchical TiO_2 micro/nanostructures to produce plasmonic TiO_2/Ag substrates as shown in Fig. 2. The Ag deposition process does not change the morphology distinctly if only seeing from the low magnification SEM images. But we can clearly see that Ag NPs get deposited on the surface of one dimensional nano-structure in higher magnification SEM images (Fig. 2c, f).

The XRD result of TiO_2/Ag is shown in Fig. 3a, which confirmed that TiO_2 nanorods are composed of anatase (JCPDS card 21-1272) and rutile phases (JCPDS card 21-1276). The diffraction peaks of TiO_2 remained unchanged after deposition of Ag NPs on the nanostructure surface (comparison of XRD results between Figs. S2d and 3a), as the anatase and rutile phase is determined by the annealing of $H_2Ti_2O_5{\cdot}H_2O$ [29,30]. On the other hand, XRD spectrum of TiO_2/Ag also contains four additional peaks attributed to Ag (111), (200), (220) and (311) planes (JCPDS card 4-0783), although the intensity of Ag peaks was relatively smaller due to the small quantity of Ag on the surface of TiO_2 nanorods [9].

XPS was also used to further determine the composition of TiO_2/Ag hierarchical micro/nanostructured substrate. In the Ti 2p spectrum (Fig. 3b), the peaks of Ti $2p_{1/2}$ and Ti $2p_{3/2}$ were centered at 464.3 eV and 458.6 eV with a spin energy separation of 5.7 eV, which is characteristic of TiO_2, being consistent with the previous reports [31,32]. The characteristic doublet peaks for Ag in Fig. 3c were also observed at binding energies of 368.1 eV and 374.1 eV for Ag $3d_{5/2}$ and Ag $3d_{3/2}$ respectively, with a spin energy separation of 6 eV, which confirm the presence of zero-valent Ag in Ag/TiO_2 composites [31,32]. For O 1s spectrum in Fig. 3d, the peaks at 530.2 eV is assigned to the lattice oxygen corresponding to TiO_2, along with a shoulder at 531.8 eV due to some absorbed oxides or a mixture of hydroxyl groups on the surface of TiO_2. The XPS results also further demonstrate that Ag NPs with good state have been loaded on the surface of TiO_2.

To demonstrate the role of microstructures in the SERS performance of TiO_2/Ag, the similar morphology of nanostructures are fabricated on the flat/laser untreated Ti surface at the same hydrothermal condition (morphology is shown in Fig. S3). All of these substrates (random structure, uniform structure, and flat surface structure) were immersed in the 10^{-5} M solution of R6G for 1 h. Raman spectra were then acquired from each sample after the surface dried naturally under the ambient environment. It's worth noting here that the SERS signal from TiO_2/Ag on femtosecond laser-structured surface was acquired from the grooved (valley) parts, as the signal is relatively weak on the cone (hill) structured surface even compared with flat surface nanostructure (Fig. S4). Based on this, Raman spectra acquired from different types of substrates are depicted in Fig. S5, with highest intensity for uniform structure (about four fold signal enhancement) is achieved, which evidently demonstrate that remarkably improved SERS activity is received here just through femtosecond laser structure adjustment. Here, the relative strong Raman bands at 1648, 1575, 1361, 1310 and 1187 cm^{-1} are ascribed to the C—C stretching modes, while 776 cm^{-1} belongs to out-of-plane bending motion of C—H of the xanthene skeleton [8].

On the other hand, the higher performance positions are in the valleys means that we just need to focus on the lowest part of these microstructures under optical microscope and can get higher signal much easier (detailed optical images during measurement are shown in Fig. S6). Based on this strategy, the reproducibility of the as-prepared SRES substrates were tested by randomly collecting signal from 5 positions of the two different structures. As can be seen from Fig. 4, SERS intensity at the different position is similar for uniform structure, which demonstrates that the TiO_2/Ag on uniform structure exhibited better reproducibility and reliability as SERS substrates than random structure. The femtosecond laser processing is a unique and scalable method for precise fabrication of microscale structure with good uniformity to get higher site predictable SERS substrate. This means that large area SERS substrates with improved reproducibility at all the bottom parts can be achieved in the near future.

The improved SERS performance of uniform hierarchical micro/nanostructured TiO_2/Ag substrate compared to other structures may be attributed to the following reasons. Firstly, electromagnetic field enhancement near the tips has been shown to be larger than other locations [11], and our method provides a good way to produce a large amount of tightly distributed tipped nanostructures. Schematic in Fig. 5a is used to clearly illustrate why SERS performance for different structures or at different positions is different. As the TiO_2/Ag nanostructure distribution of “flower-like” structures on the hill part is even more sparsely than a flat surface, thus producing a lower SERS signal because of the lower tip structure density. On the contrary, the tip structure density is higher in the valleys (smaller tip to tip distance), this will lead to a larger SERS signal within it. Secondly, many types of

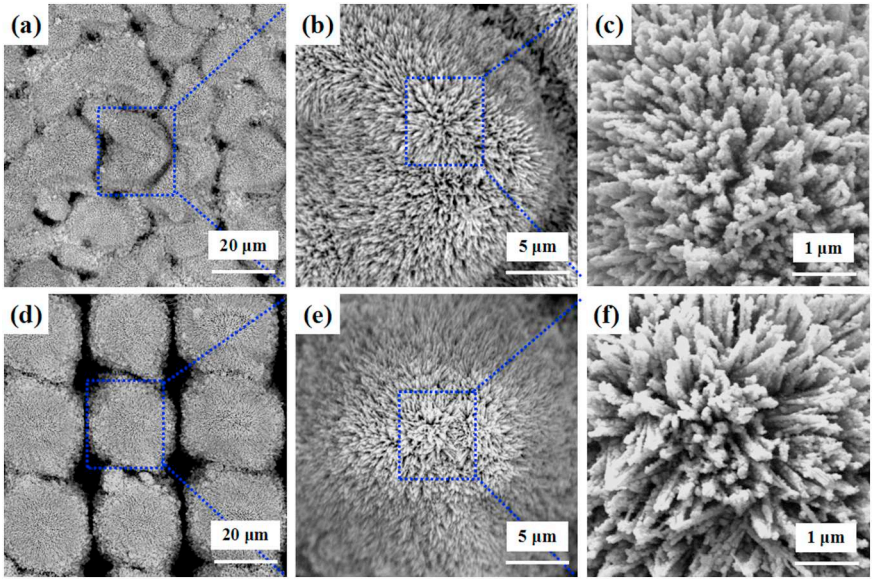

Fig. 2. SEM images for different types of TiO_2/Ag. (a, b, c) random structure, (d, e, f) uniform structure.

research have revealed that larger surface area of hierarchical structure can not only adsorb a larger number of probe molecules but also create an extensive amount of localized surface plasmons and 'hot spots' [18,33–35]. Finally, the excitation laser light can be efficiently used due to the closely distributed TiO_2/Ag tip structures [17,34,35]. All of these factors are beneficial for the improved SERS sensitivity on the hierarchical structure surface.

In order to clearly and quantitatively demonstrate the site predictability for optimal SERS signal, Raman mapping images of different Z positions (Z = 0 μm and − 10 μm corresponding to the top and bottom of the structure respectively) generated at SERS intensity corresponding to the 776 cm^{-1} of R6G are shown in Fig. 5b and c. We can see that SERS enhancement factor in the valleys is significantly larger than those at hills, which also proved that measurements in Fig. 4 is the relative better performance positions. For a traditional SERS substrate, the maximum signal is often found after extensive searching and the optimal site predictability is lacking. But in our results, we just need to search in the valleys as these are the relatively higher performance positions. Quantitatively, we calculated that the higher performance positions (red color areas) is about 54.1% and 27.6% of the whole area for Z = 0 μm and − 10 μm respectively. This means that the maximum signal can be found more easily, as we only need to search 27.6% of the whole area when focus at the bottom part of the structure.

We believe that larger SERS enhancement at valleys is combined effect of localized surface plasmon resonance (LSPR) enhancement due to higher density of nanostructures (i.e. smaller tip to tip distance) and

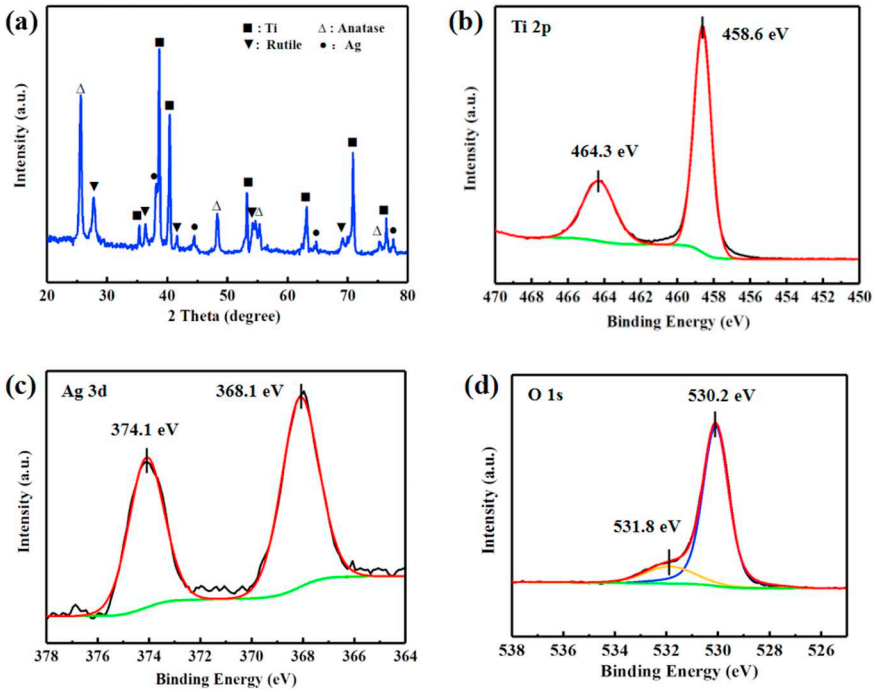

Fig. 3. XRD results and XPS spectra of TiO_2/Ag nanocomposites. (a) XRD results, (b) high-resolution XPS spectrum of Ti, (c) high-resolution XPS spectrum of Ag, (d) high-resolution XPS spectrum of O.

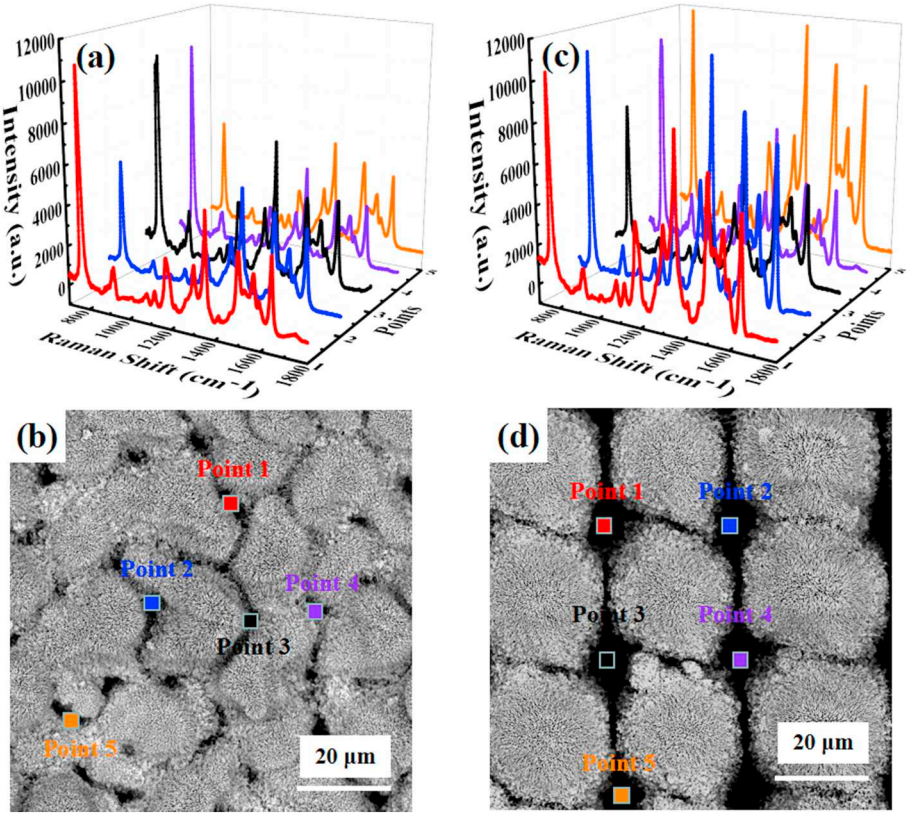

Fig. 4. SERS performance reproducibility of laser fabricated structures at different positions. (a, b) random structure, (c, d) uniform structure.

accumulation of larger amount of analyte molecules at those sites. Accumulation of probe molecules at preferred or known sites (valleys here) would have ability to achieve zepto-molar (10^{-21} M) sensitivity through increase in concentration of analyte solution via self-evaporation of solvent molecules. This functionality would either require ultra-small volume of analyte solution (most of the solution get localized at the sites of maximum enhancement i.e. at valleys) or can detect analyte molecules with zepto-molar concentration. Due to spatial variation in surface topography, grooves and hill type structures of our SERS substrate, it is not possible to decouple these two phenomena to independently study each one's contribution in SERS enhancement.

To further evaluate the SERS enhancement and analytical capability of the substrates, TiO_2/Ag substrate with uniform structure was immersed for 1 h in a series of highly diluted R6G analyte solutions with different concentrations. Under the same measurement conditions, Raman spectra were collected successively from 10^{-14} to 10^{-6} M (Fig. 6) solutions. And we can see the spectral intensity decreases here as with the R6G solution concentration decreased, but it is still highly acceptable for Raman signal recognition acquired from 10^{-14} M solution for the main fingerprint peaks in each spectrum still can be facilely identified. We can also obviously recognize these enhanced peaks acquired from 10^{-12} M and 10^{-14} M solution through the magnified view in Fig. S7. The enhancement factor (EF) of the uniform structure was estimated according to the formula $EF = (I_{SERS} / I_{Raman}) / (N_{SERS} / N_{Raman})$ [32,33]. Here, I_{SERS} stands for the intensities of the as-prepared SERS substrate and I_{Raman} stands for the Raman intensity of analyte concentration on a flat silica substrate. These data are directly obtained from the experiment. N_{SERS} and N_{Raman} are the number of R6G molecules illuminated by the laser focus spot under normal Raman and SERS conditions, respectively. In our experiment, the normal Raman spectrum was obtained by dropping 10^{-1} M R6G ethanol solution on silica substrate and dried in air. The SERS spectrum was acquired from 10^{-10} M R6G (as shown in Fig. S8). The value of EF for hierarchical nano/microstructured TiO_2/Ag substrate can reach to the order of 10 [9], which is comparable to the pure noble metal substrates and stands out in related femtosecond laser-based fabrication method [27–30]. (detailed EF calculate method is shown in Supporting information).

In the end, recycling feature is highly desirable for any type of SERS substrate to reduce their cost. Since TiO_2 (especially anatase crystal form) is an excellent photo-catalyst for the degradation of pollutants adsorbed on their surface under light irradiation, it can also be used as catalyst for the degradation of probe molecules adsorbed on its surface and act as recycling SERS substrate. To demonstrate whether our hierarchical structure still possesses this kind of advantage, recycling SERS performance is measured for the substrate. We can clearly see the intensity of Raman spectra decrease with the increase of irradiation time (Fig. S9,), which proves the degradation of R6G on TiO_2 surface. In recycled experiments for more than once, the as-prepared TiO_2 based SERS substrate also exhibits good property. Fig. 7 shows the SERS spectra acquired from 10^{-6} M R6G recorded before and after each cyclic light irradiation treatment, which indicates that the substrates can be used as a SERS substrate with high reproducibility and stability. On the other hand, laser-induced microstructures can also improve surface light utilization performance by multiple reflections of the incident light inside the surface structures [11]. This may provide us a new idea to improve the recycling performance through structure design.

4. Conclusions and future perspectives

In summary, we have successfully fabricated hierarchical micro/nanostructured TiO_2/Ag with different densities of micron and nano-sized structures by femtosecond laser structuring coupled with NaOH hydrothermal method. The as-prepared hierarchical structured TiO_2/Ag on Ti substrate exhibited enhanced SERS sensitivity than one-dimensional nanostructure on flat surface grow by the same chemical treatment. Meanwhile, reproducibility performance of the SERS substrate can be easily improved just through adjusting femtosecond laser-

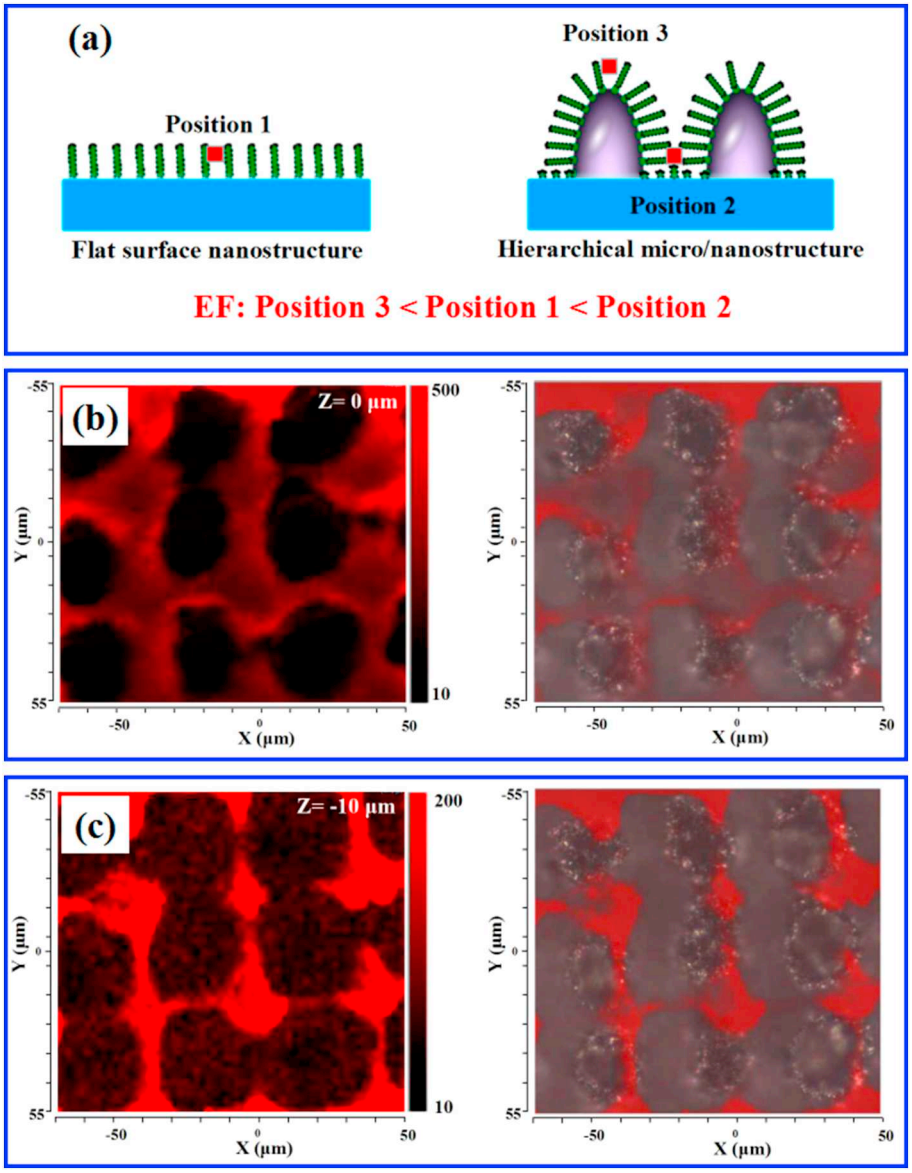

Fig. 5. Schematic of SERS improvement for different structures (a) and SERS mapping of uniform structure at different Z position (b, c) measured at 776 cm^{-1}.

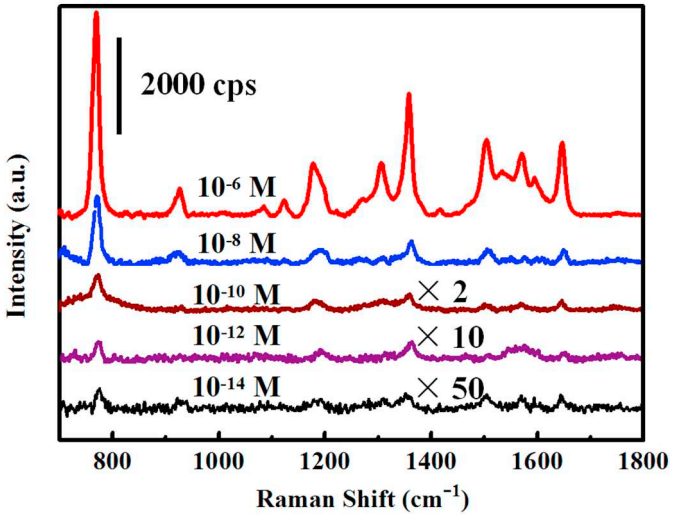

Fig. 6. Raman spectra acquired from the uniform structure after immersed in different concentrations of R6G solution.

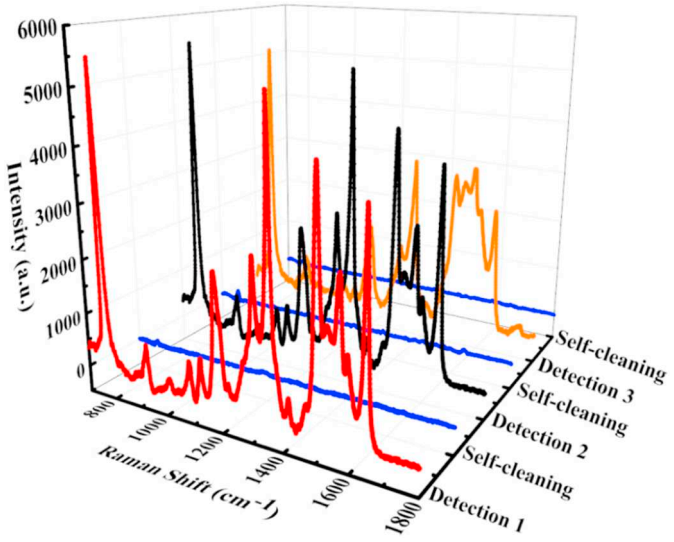

Fig. 7. Recycling performance of uniform structure after its immersion in 10^{-6} M R6G solution and degradation for 3 times.

induced microstructure to uniform arrays. Specially, enhancement factor of uniform arrays in the valleys is significantly larger than those at hills, which provide a facile solution to select out the optimal SERS performance positions of an unknown substrate. If surface of SERS substrate is not properly protected, its performance would degrade over time due to its interaction with atmospheric molecules such as sulfur/oxygen. Deposition of a protective dielectric layer on TiO_2/Ag surface would maintain plasmonic properties of Ag to increase durability of SERS substrates for their prolonged operation. The novelty of our presented work by inducing femtosecond laser could imply a potential approach to enhance the site predictability for other substrates in addition to a significant signal enhancement.

Acknowledgements

The authors acknowledge the financial supports from National Key R&D Program of China (2017YFB1104700), National Natural Science Foundation of China (11674178, 51675013), Bill & Melinda Gates Foundation (OPP1119542) of USA, and Natural Science Foundation of Tianjin City (17JCZDJC37900).

Appendix A. Supplementary data

Supplementary data to this article can be found online at https://doi.org/10.1016/j.apsusc.2019.01.257.

References

[1] S. Nie, S.R. Emory, Science 275 (1997) 1102.
[2] J.P. Camden, J.A. Dieringer, Y. Wang, D.J. Masiello, L.D. Marks, G.C. Schatz, R.P.V. Duyne, J. Am. Chem. Soc. 130 (2008) 12616.
[3] V.V. Thacker, L.O. Herrmann, D.O. Sigle, T. Zhang, T. Liedl, J.J. Baumberg, U.F. Keyser, Nat. Commun. 5 (2014) 3448.
[4] L. Xu, W. Yan, W. Ma, H. Kuang, X. Wu, L. Liu, Y. Zhao, L. Wang, C. Xu, Adv. Mater. 27 (2015) 1706.
[5] X.F. Zhang, M.Q. Zou, X.H. Qi, F. Liu, X.H. Zhu, B.H. Zhao, J. Raman Spectrosc. 41 (2010) 1655.
[6] K. Liu, Y. Bai, L. Zhang, Z. Yang, Q. Fan, H. Zheng, Y. Yin, C. Gao, Nano Lett. 16 (2016) 3675.
[7] X. Liu, J. Iocozzia, Y. Wang, X. Cui, Y. Chen, S. Zhao, Z. Li, Z. Lin, Energy Environ. Sci. 10 (2017) 402.
[8] X. Li, G. Chen, L. Yang, Z. Jin, J. Liu, Adv. Funct. Mater. 20 (2010) 2815.
[9] H. Dai, Y. Sun, P. Ni, W. Lu, S. Jiang, Y. Wang, Z. Li, Z. Li, Sensors Actuators B Chem. 242 (2017) 260.
[10] G. Barbillon, V.E. Sandana, C. Humbert, B. Belier, D. Rogers, F. Teherani, P. Bove, R. McClintockd, M. Razeghi, J. Mater. Chem. C 5 (2017) 3528.
[11] F. Hui, X.Z. Chang, L. Luo, M.Z. Yong, J.X. Hai, Biosens. Bioelectron. 64 (2015) 434.
[12] X.X. Han, W. Ji, B. Zhao, Y. Ozaki, Nanoscale 9 (2017) 4847.
[13] W. Zhou, B.C. Yin, B.C. Ye, Biosens. Bioelectron. 87 (2017) 187.
[14] M. Chirumamilla, A. Toma, A. Gopalakrishnan, G. Das, R.P. Zaccaria, R. Krahne, E. Rondanina, M. Leoncini, C. Liberale, F.D. Angelis, E.D. Fabrizio, Adv. Mater. 26 (2014) 2353.
[15] H. Liu, Z. Yang, L. Meng, Y. Sun, J. Wang, L. Yang, J. Liu, Z. Tian, J. Am. Chem. Soc. 136 (2014) 5332.
[16] H. Zhao, J. Jin, W. Tian, R. Li, Z. Yu, W. Song, Q. Cong, B. Zhao, Y. Ozaki, J. Mater. Chem. A 3 (2015) 4330.
[17] Q. Zhang, Y.H. Lee, I.Y. Phang, C.K. Lee, X.Y. Ling, Small 10 (2014) 2703.
[18] Q. Ding, H. Zhou, H. Zhang, Y. Zhang, G. Wang, H. Zhao, J. Mater. Chem. A 4 (2016) 8866.
[19] S.L. Kleinman, R.R. Frontiera, A.I. Henry, J.A. Dieringer, R.P. Van Duyne, Phys. Chem. Chem. Phys. 15 (2013) 21.
[20] M. Yilmaz, M. Erkartal, M. Ozdemir, U. Sen, H. Usta, G. Demirel, ACS Appl. Mater. Interfaces 9 (2017) 18199.
[22] X. Tang, W. Cai, L. Yang, J. Liu, Nanoscale 5 (2013) 11193.
[23] P. Zuo, L. Jiang, X. Li, B. Li, Y. Xu, X. Shi, P. Ran, T. Ma, D. Li, L. Qu, Y. Lu, C.P. Grigoropoulos, ACS Appl. Mater. Interfaces 9 (2017) 7447.
[24] S. Li, H. Zhang, L. Xu, M. Chen, Opt. Express 25 (2017) 16204.
[25] Y. Bellouard, E. Block, J. Squier, J. Gobet, Opt. Express 25 (2017) 9587.
[26] D. Wang, Nat. Photonics 2 (2008) 219.
[27] A. Wang, L. Jiang, X. Li, Q. Xie, B. Li, Z. Wang, K. Du, Y. Lu, J. Mater. Chem. B 5 (2017) 777.
[28] T. Huang, J. Lu, R. Xiao, Q. Wu, W. Yang, Appl. Surf. Sci. 403 (2017) 584.
[29] M. Chu, Y. Tang, N. Rong, X. Cui, F. Liu, Y. Li, C. Zhang, P. Xiao, Y. Zhang, Mater. Des. 97 (2016) 257.
[30] J.Y. Liao, B.X. Lei, H.Y. Chen, D.B. Kuang, C.Y. Su, Energy Environ. Sci. 5 (2012) 5750.
[31] K.C. Hsu, D.H. Chen, ACS Appl. Mater. Interfaces 7 (2015) 27571.
[32] Q. Huang, J. Li, W. Wei, Y. Wu, T. Li, RSC Adv. 7 (2017) 26704.
[33] X. He, Y. Liu, X. Xue, J. Liu, Y. Liu, Z. Li, J. Mater. Chem. C 5 (2017) 12384.
[34] D. Yang, H. Cho, S. Koo, S.R. Vaidyanathan, K. Woo, Y. Yoon, H. Choo, ACS Appl. Mater. Interfaces 9 (2017) 19092.
[35] A.Y. Vorobyev, C. Guo, Laser Photonics Rev. 7 (2013) 385.